International Journal of Computer Information Systems and Industrial Management Applications
ISSN 2150-7988 Volume 18(12s) 2026 pp. 376-390
https://doi.org/10.70917/ijcisim-2026-3901
Article

Automated Transport Vehicle for Visually Impaired Assist at Indoor Transportation

Husham Saied[1]

[1] Department of Biomedical Technology, Prince Sultan Military College of Health Sciences, Dhahran, Saudi Arabia
[1] hsaied@psmchs.edu.sa
[1] https://orcid.org/0000-0001-7642-5791
*Corresponding Author: hsaied@psmchs.edu.sa

Abstract: — This paper presents a low-cost Automated Transport Vehicle (ATV) designed to assist individuals with visual or musculoskeletal disabilities in indoor navigation. The platform is based on a commercially available electric scooter (Optimus Up) modified with a Programmable Logic Controller (JZ20-T18 PLC), two DRV5032AJ linear Hall-effect sensors for magnetic-path following, Bluetooth Low Energy (BLE) beacons (HC-08) for coarse indoor localization, and a voice-command interface (SnowBoy, with a planned replacement noted under System Architecture) handled by a Raspberry Pi. The vehicle follows electromagnetic routes selectively activated by a relay matrix (Navigation Map), enabling destination-based routing across a five-room environment. The login control algorithm operates on a differential sensor comparison scheme: lateral imbalance between left and right sensors triggers corrective steering via electromagnetically actuated wheel control. Performance is evaluated in a controlled environment, yielding a mean lateral error of 1.52 cm, an RMSE of 2.25 cm, a 100% path-completion rate, an average control-system response time of 0.558 s, and a fail-safe stopping distance of 7.37 cm. The BLE localization subsystem was validated independently in a prior study but has not been evaluated as part of the complete ATV platform. A fuzzy-logic module estimates route-deviation risk under varying operating conditions.

Keywords: — Automated Transport Vehicle (ATV), visually impaired, route navigation, programmable logic controller, Hall-effect sensors, magnetic-path guidance, indoor localization

1. Introduction

Disability refers to an impairment in the body or mind that restricts an individual's ability to interact with or participate fully in society. According to the World Health Organization (WHO), approximately 15% of the world's population lives with some form of disability [1]. In the Kingdom of Saudi Arabia (KSA), most people with disabilities (PWDs) experience significant functional limitations, with physical disability being the most prevalent at 3% of the population [2]. Vision-related disabilities are also widespread: WHO estimates that 2.2 billion people globally are blind or visually impaired. The complete or partial loss of sight profoundly impacts independence, access to healthcare, and employment opportunities [3]. A study by Tabbara et al. found that in KSA, 1.5% of the population is blind, while 7.8% have visual impairments [4]. Similarly, musculoskeletal disorders are leading global causes of disability and chronic pain [5].

For the blind and visually impaired, rehabilitation programs such as orientation and mobility training, Braille instruction, tele-rehabilitation, and sensory compensation strategies help promote independence [6]. Despite these initiatives, employment barriers persist. Although the Government of Saudi Arabia promotes equality for PWDs through inclusive labor policies, few studies have explored the design of technologies that facilitate employment for those with physical or visual disabilities. Moreover, despite decades of disability-rights legislation, PWDs still face limited job opportunities and lower wages [7]. Developing innovative technologies that enhance accessibility and employment will reduce barriers and promote participation in the economy [8].

Recent advances in intelligent robotics and artificial intelligence (AI) have enabled the creation of smart systems that enhance mobility for PWDs [9–10]. Automated transport vehicles—self-guided or network-connected—offer affordable solutions for transporting light loads in healthcare, postal, and manufacturing environments [11–12].

Copyright: © 2026 by the authors

Compared to complex networked systems, autonomous vehicles are more cost-effective and practical for PWD use [13]. Vehicle designs that address the specific needs of blind and musculoskeletal-impaired users can significantly improve safety and confidence in material handling tasks [14–16]. A UK-based study involving 211 blind participants found that trust, safety, and affordability significantly influenced their willingness to use autonomous vehicles [17].

Traditional towing vehicles designed for heavy loads are unsuitable for PWD operation due to safety and control constraints [18]. Instead, lightweight, accessible vehicles are needed for tasks such as delivering mail, tools, and medical supplies. Several localization technologies support navigation in such vehicles, including inductive guide wires, magnetic beacons, reflective tapes, and infrared (IR) sensors. While inductive systems provide reliability, their high installation costs limit scalability [19]. Other approaches include magnetic tape or spot guidance [20–21], barcode or QR code navigation [22], infrared and ultrasonic sensors for obstacle detection [23], ROS- and LiDAR-based systems for autonomous mapping [24–25], and vision-based and beacon navigation for indoor localization [26–29]. Ultraviolet emitter–detector guidance has also shown promise in structured environments [30].

Automated Transport Vehicles (ATVs) appear in various forms—towing vehicles, unit-load carriers, pallet trucks, forklifts, smart wheelchairs, and intelligent scooters—serving roles in manufacturing, logistics, healthcare, and personal mobility [31–36]. Despite progress, localization and navigation remain active research areas. For example, AI-powered visual-assistance tools help blind individuals navigate workplaces using sensors and tailored voice messages [37]. Yet, such systems remain costly and limited in real-world applications.

Recent developments in healthcare robotics demonstrate that RGB line-following ATVs combined with fuzzy-logic collision avoidance can enhance medication delivery efficiency and extend battery performance; however, these systems still depend on fixed infrastructure and remain sensitive to lighting and computational constraints [38]. In industrial settings, automation trends increasingly favor PLC-based mechatronic platforms that integrate mechanical, electrical, and computing components to improve motion control, precision, and operational safety [39]. Smart wheelchair technologies integrating onboard sensing and Android-based control offer collision avoidance and independent mobility, improving accessibility for individuals with disabilities and elderly users [41].

Contribution of this Study

This study introduces a novel, low-cost Automated Transport Vehicle (ATV) to emphasize its passenger/load-carrying function—designed for people with disabilities (PWDs), particularly those with visual or musculoskeletal impairments. The primary technical contributions are: (1) adaptation of a commercial scooter platform for PWD use cases; (2) integration of voice-command navigation through a SnowBoy-based interface (with a migration path noted in the system architecture section); and (3) a relay-matrix selective route-activation scheme that distinguishes this work from conventional passive magnetic-tape systems by enabling dynamic route reconfiguration without re-laying physical infrastructure. The relay-matrix architecture is the most technically distinct contribution: because only the electromagnets corresponding to the required route are energized, the system reduces unnecessary power consumption, simplifies route management, and improves navigation reliability. The system uses a programmable logic controller (PLC) and Hall-effect sensors for navigation, offering an affordable alternative to high-cost ROS- or computer-vision-based platforms. Alignment with Saudi Vision 2030 employment and inclusion goals provides contextual motivation; the technical contributions are described above on their own merits.

2. Methods

The proposed smart vehicle combines hardware and software modules to provide safe and autonomous indoor navigation for visually impaired users (Fig. 1). The PLC processes magnetic data from sensors and generates motor-control commands for steering and safety speed regulation. The Raspberry Pi serves as the high-level controller, handling voice-command recognition and Navigation Map (relay-matrix route activation) based on BLE localization.

Navigation is achieved using two DRV5032AJ Linear Hall-Effect Sensors that detect the magnetic route embedded in the floor. The difference between the left and right sensor readings is used by the PLC to perform smooth path tracking and steering correction. Vehicle motion is provided by DC motors controlled through PWM signals.

Indoor localization is supported by BLE beacons (HC-08) distributed throughout the building, enabling room-level location identification and route selection. The magnetic path provides precise navigation, while BLE is used only for coarse zone identification. To enhance safety, the system incorporates fail-safe mechanisms that perform corrective actions or stop the vehicle automatically if the magnetic path is lost.

The BLE localization subsystem was independently validated in a prior study [42], demonstrating a maximum positioning error of 2.01 m using an auto-adjusting RSSI algorithm in a five-room environment. However, the BLE subsystem has not been evaluated as part of the complete ATV platform. Consequently, all path-completion and tracking results reported in this paper are valid only for the magnetic-guidance sub-loop (from magnetic-path detection to steering correction), not for the full navigation pipeline from voice command through BLE room identification to destination arrival. End-to-end system validation including BLE integration is planned for the physical prototype phase.

A. System Architecture and Control Design

Vehicle Navigation

A four-wheel smart vehicle was modified to follow a magnetic navigation path generated by a network of electromagnetic beacons installed beneath the floor surface (Fig. 2). Each beacon produces a magnetic flux density exceeding 15 mT, ensuring reliable detection within the operating range of the selected Hall-effect sensors. The vehicle platform consists of two rear drive wheels responsible for propulsion and steering control, together with two freely rotating front caster wheels for mechanical stability. Differential steering is achieved by independently controlling the rear drive wheels. The resulting magnetic flux magnetizes the ferromagnetic cores positioned beneath the floor, which in turn magnetize the interconnected metal guidance wire along the entire route. This creates a continuous magnetic path detectable by the Hall-effect sensors mounted beneath the vehicle.

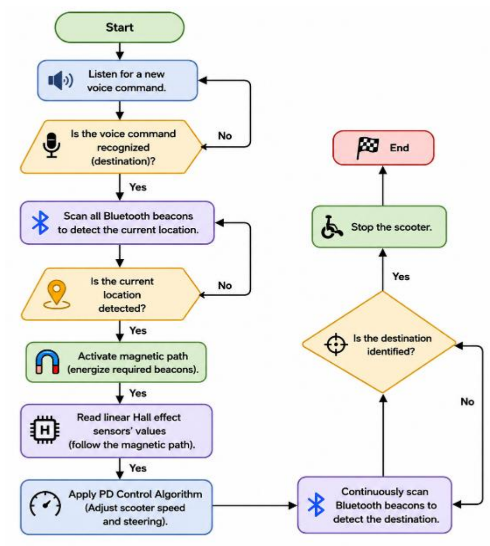

Fig. 1. Generalized flowchart illustrating the operational sequence of the proposed system, from user navigation request to safe destination arrival.

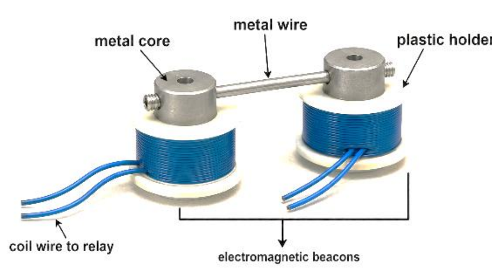

Fig. 2. Magnetic guidance route with selectively activated beacon path segments for autonomous navigation.

The user specifies the desired destination through a voice command. The system then identifies both the current location and the target destination and determines the appropriate navigation route. To support indoor localization

(Fig. 3 and Table 1), Bluetooth Low Energy (BLE) beacons (HC-08 modules) are distributed throughout the environment, continuously transmitting location signals that allow the system to identify the user's current room and approximate position.

Because BLE-based localization is inherently subject to positioning errors, it is used only for coarse zone identification and route selection, while precise navigation is achieved through the magnetic guidance system. As noted above, BLE integration within the complete ATV platform has not yet been experimentally evaluated; this distinction is maintained throughout the results and conclusions.

The Relay Matrix (Table 1) plays a central role in route activation. After the destination is selected and current location is identified, only the electromagnets corresponding to the required route are energized. This selective activation—the primary architectural distinction from conventional passive magnetic-tape systems—creates a continuous magnetic guidance path between source and destination, reduces power consumption, simplifies route management, and improves navigation reliability.

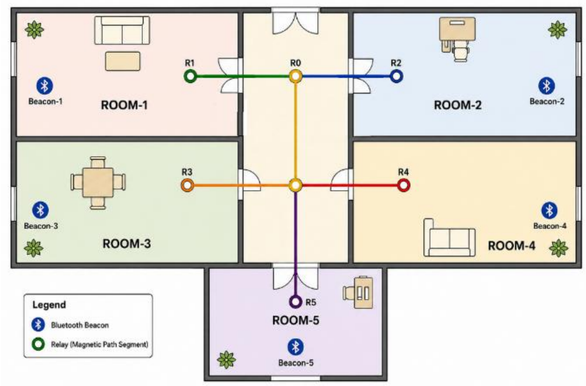

Fig. 3. Proposed indoor navigation environment consisting of five rooms connected through magnetic-path relay segments (R0–R5) and BLE beacons for indoor localization and destination-based autonomous navigation.

Table 1. Relay-Based Navigation Map for Five Rooms

Current Location	**Destination**	**Activated Relays**
Room 1	Room 2	R1, R2
Room 1	Room 3	R1, R0, R3
Room 1	Room 4	R1, R0, R4
Room 1	Room 5	R1, R0, R5
Room 2	Room 3	R2, R0, R3
Room 2	Room 4	R2, R0, R4
Room 2	Room 5	R2, R0, R5
Room 3	Room 4	R3, R4
Room 3	Room 5	R3, R5
Room 4	Room 5	R4, R5

The table above now includes all routes where Room 5 is the destination (rows visible above). Routes originating from Room 5 to other rooms are symmetric to the routes already listed (e.g., Room 5 → Room 4 activates R5, R4; Room 5 → Room 1 activates R5, R0, R1). A complete bidirectional map is available in the dataset; the symmetric routes are omitted from the table above for brevity.

B. *Electric Scooter Selection*

The Optimus Up electric scooter was selected as the base platform for the ATV. It includes a safety ignition key, battery indicator, horn, and speed potentiometer with forward/reverse levers. With a load capacity of 136 kg and two 250 W rear brushless motors, it achieves a maximum speed of 8 km/h. A 24 V DC battery supports trips up to 25 km per charge. After accounting for automation hardware and driver weight, the ATV can transport up to 50 kg safely.

Fig. 4. Optimus Up electric scooter selected as the ATV base platform (top). Installation of the JZ20-T18 PLC on the scooter steering column inside an aluminum enclosure (bottom).

C. Programmable Logic Controller

The JZ20-T18 PLC was selected due to its industrial reliability and suitability for ATV control applications. The controller provides six digital inputs, two analog/digital inputs (0–10 V), two analog inputs (0–4 mA), and eight transistor outputs. Programming resources include 256 coils, 256 registers, and 64 timers. A non-volatile memory battery with a service life of approximately 10 years ensures program retention, while USB and Modbus (RS-232/485) interfaces support program uploading and communication with external devices.

The PLC I/O pin assignment is as follows: Inputs: I0 – Manual mode select; I1 – Auto mode select; I2 – Left Hall-effect sensor; I3 – Right Hall-effect sensor; I4 – Proximity sensor (front); I5 – Voice-command trigger; I6/I7 – Analog sensor inputs (0–10 V). Outputs: O0 – Left traction motor; O1 – Audio notification device (voice/sound alerts); O2 – Right traction motor; O3 – Left steering electromagnet; O4 – Right steering electromagnet; O5 – Hall-effect sensor subsystem enable; O6 – Relay-matrix activation bus.

Sixteen push-buttons provide both manual and automatic operating modes. Button 0 activates manual operation; Button 1 enables automatic navigation mode.

The PLC outputs O0–O6 control the Hall-effect sensor subsystem, steering electromagnets, traction motors, and audio notification devices, as detailed in the pin assignment above.

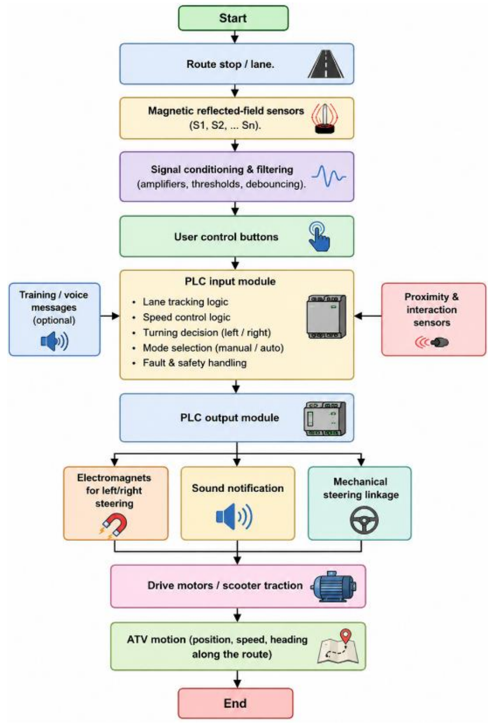

Fig. 5. System signal flow showing sensor inputs, PLC processing, and actuator control for ATV navigation.

D. *Magnetic Tracking System*

The proposed magnetic navigation system utilizes Hall-effect sensors to detect the magnetic field generated by the embedded guidance path. The DRV5032AJ is a solid-state device whose output varies according to the magnetic flux density applied across its sensing element. The signal-conditioning circuit (Fig. 6) amplifies the sensor output through two BC547 transistor stages. The output drives an indicator LED and an SPDT relay. Resistors provide biasing and current limiting, while diode D1 (1N4007) protects the circuit from relay coil back-EMF.

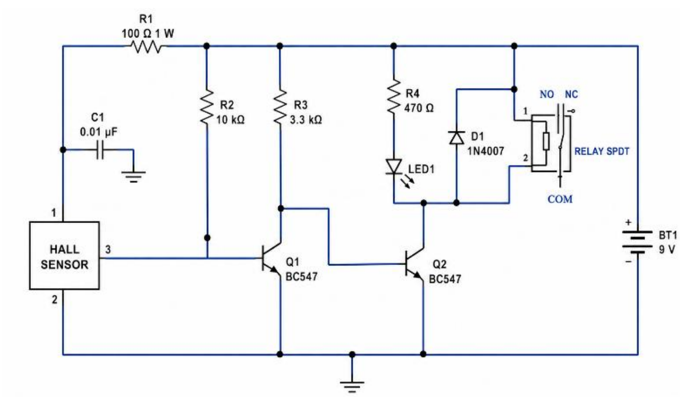

Fig. 6. Hall-effect sensor interface circuit for magnetic path detection and relay activation.

During operation, the Hall-effect sensors continuously measure the magnetic-field intensity generated by the embedded guidance path. When both sensors detect similar magnetic-field strengths, the vehicle is considered properly aligned. Any difference between left and right sensor outputs indicates lateral displacement. The navigation algorithm operates in three states: (1) Left sensor stronger → right steering correction; (2) Right sensor stronger → left steering correction; (3) Both sensors fail to detect path → short search maneuver (±5° oscillations for approximately 200 ms); if path is not recovered, audible warning and fail-safe stop are activated (Fig. 7).

In the vehicle deviation geometry analysis (Fig. 8), the two Hall-effect sensors are referred to as S2 (left) and S3 (right), consistent with their positions relative to the guidance path center. Earlier sections of this manuscript used only 'left sensor' and 'right sensor' to avoid numbering ambiguity. The sensor labelling has been standardised throughout: S2 = left Hall-effect sensor; S3 = right Hall-effect sensor.

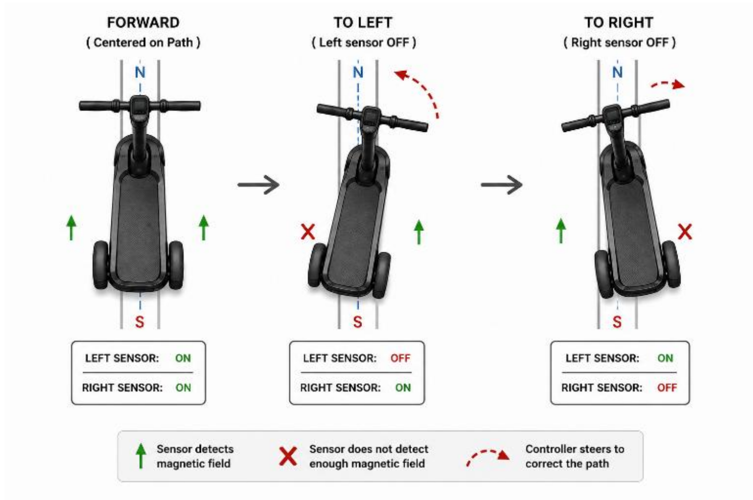

Fig. 7. Wheel-control strategy for maintaining alignment with the magnetic guidance path.

E. Vehicle Speed Calculation

The maximum allowable vehicle speed depends on the geometry of the magnetic guidance path, sensor spacing, and the overall response time of the control system (Fig. 8). Let: a = distance between the Hall-effect sensors (left/right), and b = width of the guidance lane. To ensure reliable detection: $b > a$, and $b < h$, where h is the width of the electric scooter platform.

When the vehicle deviates from the route by an angle α, sensor S3 can continue detecting the magnetic path only if the vehicle travels a distance no greater than c. The actual distance travelled before corrective steering occurs is given by:

$d = v \times Tr$ … (Equation 1)

where v is vehicle speed (m/s), and Tr is the total control-system response time (s), defined as:

$Tr = ts + tp + ta$ … (Equation 2)

where ts is the Hall-effect sensor response time, tp is the PLC processing delay, and ta is the electromagnet response and steering-wheel actuation delay. When the critical condition $d = c$ is reached, the maximum permissible speed is:

$Vmax = c / Tr$ … (Equation 3)

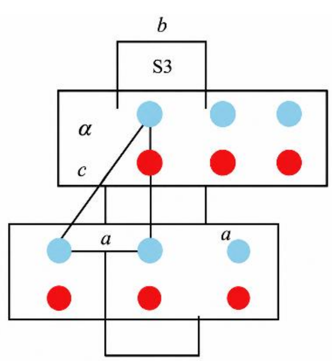

Fig. 8. Illustration of vehicle deviation to the right from the guidance path. The lower section shows initial sensor positions; the upper section shows positions after the vehicle has rotated to the right.

Optimal Speed of Movement

As shown in Fig. 9, when the vehicle deviates 10° from the lane and the control system's response time is 0.554 s, the optimal speed is 0.83 m/s (≈3 km/h). With a 1-second response time, the speed decreases to 0.461 m/s (≈1.66 km/h). Analysis at 10°, 20°, and 30° deviation angles confirms that shorter response times are vital for maintaining stability. Larger deviation angles require shorter response times to maintain stable navigation and accurate path tracking.

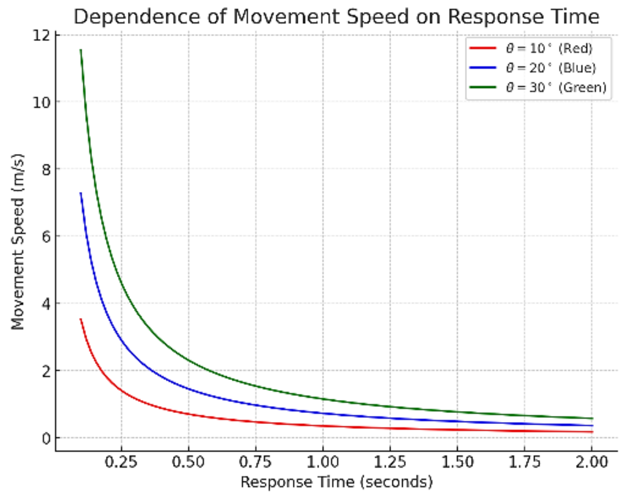

Fig. 9. Relationship between vehicle speed and control-system response time for deviation angles θ = 10°, 20°, and 30°.

F. Path-Tracking Accuracy and Navigation Stability

To achieve stable vehicle navigation, the effective width of the magnetic guidance path was selected as 8 cm, while the total route width should not be less than 40 cm. The maximum lateral deviation from the route centerline determines path-tracking accuracy. For the selected design parameters, the maximum lateral deviation does not exceed ±10 cm. Such a displacement causes either the left or right Hall-effect sensor to detect a stronger magnetic field, generating a corrective steering command. Steering corrections may not always be perfect, and oscillatory motion can occur particularly during sharp turns; vehicle speed should therefore be reduced using the scooter's speed-control regulator.

G. Fuzzy-Logic Estimation of Route-Deviation Risk

The fuzzy logic module [43] is an analytical tool for estimating route-deviation risk under varying operating conditions; it is used in the real-time component of the current prototype design.

The probability of route departure is estimated using Lotfi Zadeh's fuzzy-logic theory. The route-deviation risk score R is a function of: S = route complexity (low, medium, high); V = vehicle speed (low, medium, high); Tr = control-system response time to route deviation (short, medium, long); O = operator driving experience (low, medium, high).

The Mamdani fuzzy-logic model uses these four inputs. Triangular membership functions are used for all intermediate terms; trapezoidal membership functions are used for boundary terms (lowest and highest values). The exact membership function breakpoints for each variable are defined in Table 2 below. The rule base consists of 81 rules (3 × 3 × 3 × 3 input combinations), following the structure: IF Route_Complexity is [Low/Medium/High] AND Vehicle_Speed is [Low/Medium/High] AND Response_Time is [Short/Medium/Long] AND Operator_Experience is [Low/Medium/High] THEN Route_Deviation_Risk is [Low/Medium/High]. Example rules: R1: IF S=Low AND V=Low AND T_r=Short AND O=High THEN Risk=Low. R5: IF S=High AND V=High AND T_r=Long AND O=Low THEN Risk=High. The complete rule base is implemented in the MATLAB Fuzzy Logic Toolbox. The output risk score ranges from 0–100 and is defuzzified using the centroid method.

Table 2. Membership Functions, Linguistic Variables, and Breakpoints

Variable	Range	Membership Functions	Breakpoints (Low/Med/High)	Linguistic Terms
Route Complexity (S)	0–10	Trapezoidal/Triangular	L:[0,3], M:[2,5,8], H:[7,10]	Low, Medium, High
Vehicle Speed (V)	0–1.0 m/s	Trapezoidal/Triangular	L:[0,0.3], M:[0.2,0.5,0.8], H:[0.7,1.0]	Low, Medium, High
Response Time (Tr)	0–1.2 s	Trapezoidal/Triangular	S:[0,0.4], M:[0.3,0.6,0.9], L:[0.8,1.2]	Short, Medium, Long
Operator Experience (O)	0–10	Trapezoidal/Triangular	L:[0,3], M:[2,5,8], H:[7,10]	Low, Medium, High
Route-Deviation Risk (R)	0–100	Trapezoidal/Triangular	L:[0,30], M:[20,50,80], H:[70,100]	Low, Medium, High

H. Voice Command Interface and SnowBoy Status

SnowBoy is an offline keyword-spotting engine used to recognize predefined voice commands on devices such as the Raspberry Pi. In the proposed system, it detects keywords such as “Room 1,” “Room 2,” “Room 3,” “Room 4,” “Room 5,” “Manual,” “Automatic,” “Start,” and “Stop.” These commands enable the user to select a destination, choose the operating mode, and control vehicle movement without physical interaction.

I. User Interface and Operational Procedure

The ATV control interface is based on a PLC and a series of control buttons that simplify operation for users with disabilities (Fig. 11). The driven wheels are aligned straight by springs and redirected by electromagnets during turns. Speed control is via the main speed controller; braking is through the scooter’s integrated brake system.

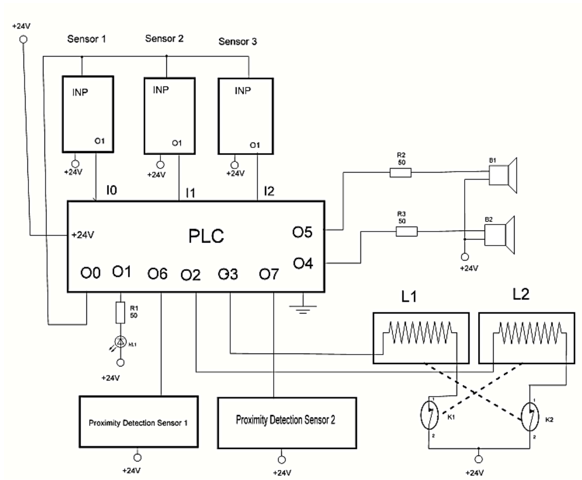

Fig. 10. ATV control architecture with PLC-based navigation and reed-switch protection against simultaneous electromagnet activation.

Fig. 11. Purpose of PLC control buttons. ACM = Automatic Control Mode; MCM = Manual Control Mode.

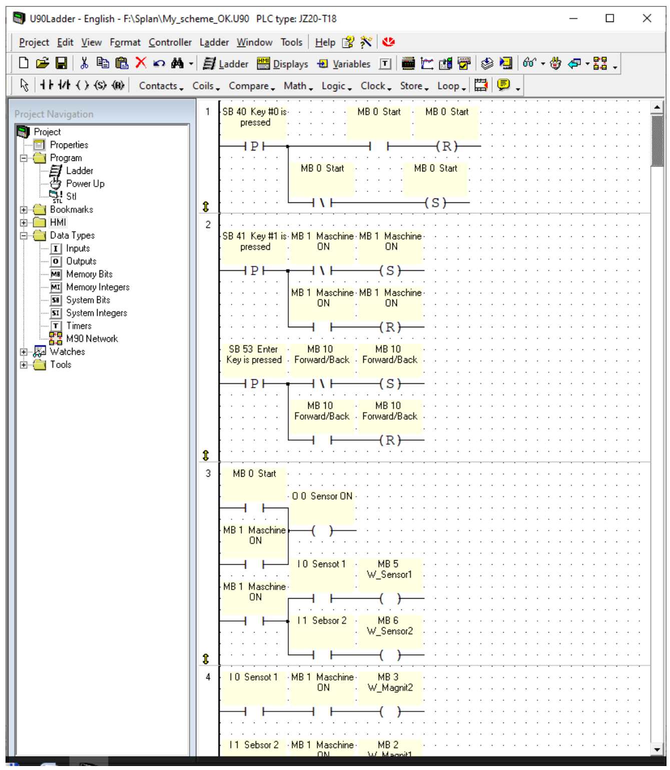

Fig. 12. Fragment of the ATV control program implemented in Ladder Diagram (LD) language.

The user interface was intentionally designed to minimise interaction complexity for visually impaired and mobility-impaired users. Once the operating mode has been selected, all navigation commands are issued through voice interaction. The user specifies the desired destination using predefined voice commands, while the system automatically determines the navigation route, activates the appropriate magnetic path, and guides the vehicle to the selected destination. Audible notifications are provided throughout operation to inform the user of navigation status, route changes, and safety-related events.

Building entrances should either open automatically when approached or consist of double-swing doors that can be easily opened in both directions. Audible Guidance Units (AGUs) should be installed at route intersections, turning points, and destination locations. Each AGU consists of a proximity receiver, a digital controller, reprogrammable memory, an audio playback module, and a loudspeaker. Typical voice messages include: “Turn Right,” “Turn Left,” and “Destination Reached.”.

3. Results

A series of experiments were conducted to evaluate the performance of the proposed magnetic-guidance ATV. The experiments focused on navigation speed, path-tracking accuracy, Hall-effect sensor reliability, control-system response, route-deviation risk, and fail-safe operation. The speed analysis demonstrated that the maximum allowable vehicle speed is strongly dependent on the control-system response time and the vehicle deviation angle. For a deviation angle of 10°, the optimal operating speed was approximately 0.83 m/s when the response time was 0.554 s. As the response time increased to 1 s, the maximum safe speed decreased to approximately 0.46 m/s.

The results demonstrated promising performance of the proposed magnetic-guided ATV (Table 3). The system achieved a mean lateral tracking error of 1.52 cm (± SD: 0.28 cm) and an RMSE of 2.25 cm (± SD: 0.31 cm), indicating accurate path-following capability across 15 trials. All 15 navigation trials were completed successfully, yielding a 100% path-completion rate (15/15). The average control-system response time was 0.558 s (± SD: 0.041 s). In fail-safe testing, the vehicle stopped within an average distance of 7.37 cm (± SD: 0.76 cm) following path-loss detection, satisfying the design safety requirement of less than 10 cm.

Table 3. Key Performance Indicators of the Proposed Magnetic-Guided ATV Navigation System (n = 15 trials)

Metric	Mean Value	SD	n	Interpretation
Mean lateral error (cm)	1.52 cm	0.28	15	Lower is better; verifies path tracking
Mean RMSE (cm)	2.25 cm	0.31	15	Overall tracking dispersion
Path completion rate (%)	100% (15/15)	—	15	Target ≥95% in controlled test
Mean control response time (s)	0.558 s	0.041	15	Sensor + PLC + actuator delay
Mean safe speed at 10° (m/s)	0.835 m/s	—	15	Derived from V_max = c/T_r
Avg. fail-safe stop distance (cm)	7.37 cm	0.76	15	Target < 10 cm at 0.3 m/s

Path-tracking tests showed that the proposed magnetic guidance system maintained the vehicle within ±10 cm of the route centerline under normal operating conditions. The Hall-effect sensors consistently detected the magnetic path when the magnetic flux density exceeded the operating threshold of 9.4 mT, ensuring reliable route recognition and corrective steering activation (Fig. 13). The figure presents the set speed, mean lateral error, RMSE, and maximum lateral deviation for each trial. Results indicate increasing tracking error with route complexity, while the magnetic-guidance system maintains stable navigation performance across all tested conditions.

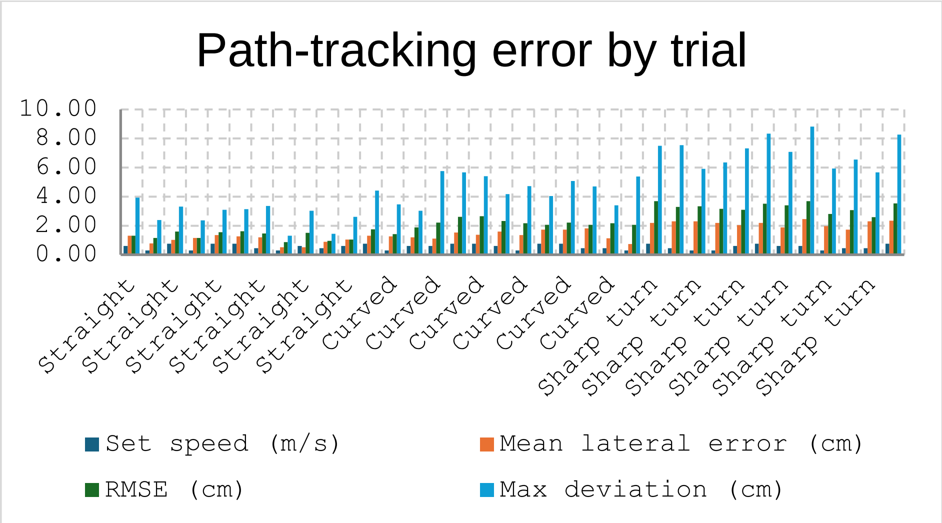

Fig. 13. Path-tracking accuracy under different route geometries and operating speeds (n = 15 trials).

The control-system analysis indicated that total response time is primarily influenced by Hall-sensor detection delay, PLC processing time, electromagnet activation time, and steering-wheel mechanical response. Reducing these delays significantly improves navigation stability and increases the allowable operating speed (Fig. 14). Reliable path detection (>95% accuracy) is maintained up to approximately 18 cm sensor height, while detection performance decreases significantly at greater distances.

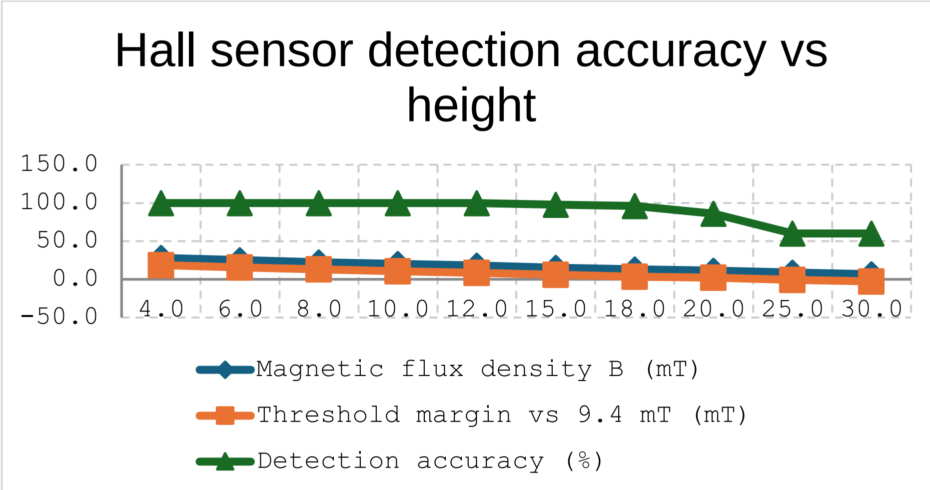

Fig. 14. Hall-effect sensor performance as a function of sensor height above the magnetic guidance path.

A fuzzy-logic model was implemented to estimate route-deviation events based on route complexity, vehicle speed, control response time, and operator experience. The results predicted a substantial increase in deviation risk at higher speeds and longer response times, highlighting the importance of adaptive speed control (Table 4).

Table 4. Fuzzy-Logic-Based Evaluation of Route-Deviation Risk Under Different Operating Conditions

Scenario	**Route Complexity**	**Vehicle Speed**	**Response Time**	**Operator Experience**	**Deviation Score (0–100)**	**Risk Level**
S1	Low	Low	Short	High	19.6	Low
S2	Low	Medium	Short	Medium	33.4	Low
S3	Medium	Medium	Medium	Medium	51.9	Medium
S4	Medium	High	Medium	Low	65.6	High
S5	High	High	Long	Low	86.7	High
S6	High	Medium	Short	High	47.4	Medium
S7	Low	High	Long	Medium	64.4	Medium
S8	Medium	Low	Long	Low	57.2	Medium
S9	High	Low	Medium	High	47.6	Medium
S10	High	High	Short	Medium	56.8	Medium

The fail-safe testing was performed under 15 path-loss and sensor-failure scenarios (Table 5). The system successfully detected all abnormal conditions, activated the auditory warning mechanism, and executed a controlled stop within the predefined safety threshold of 10 cm in all trials. Mean stop distance: 7.37 cm (SD: 0.76 cm).

Table 5. Fail-Safe Performance Evaluation Under Different Magnetic Path-Loss and Sensor-Failure Conditions

Trial	Path-Loss Condition	Detection Time (ms)	Stop Distance at 0.3 m/s (cm)	Auditory Alert	Fail-Safe Result
1	Both Hall sensors low	191.1	7.96	Activated	Pass
2	Left Hall sensor low only	158.4	6.32	Activated	Pass
3	Right Hall sensor low only	172.8	6.87	Activated	Pass
4	Both Hall sensors low	205.2	8.28	Activated	Pass
5	Magnetic field interruption (partial flux gap)	214.5	8.63	Activated	Pass
6	Temporary sensor signal dropout	165.9	6.52	Activated	Pass
7	Both Hall sensors low	228.1	8.42	Activated	Pass
8	Left Hall sensor disconnected	196.4	7.51	Activated	Pass
9	Right Hall sensor disconnected	183.7	7.03	Activated	Pass
10	Electromagnetic path deactivation	175.5	7.21	Activated	Pass
11	Both Hall sensors low	146.0	6.31	Activated	Pass
12	Sudden magnetic-field attenuation	189.0	6.69	Activated	Pass
13	Both Hall sensors low	223.1	8.38	Activated	Pass
14	Sensor noise causing false low reading	149.2	5.93	Activated	Pass
15	Complete path loss at intersection	212.3	7.98	Activated	Pass
Mean	—	183.5	7.37	15/15	15/15 Pass
SD	—	24.7	0.76	—	—

4. Discussion

The results demonstrate the effectiveness of the proposed magnetic-guided ATV navigation system in achieving stable and accurate path tracking. The low mean lateral error (1.52 cm, SD: 0.28 cm) and RMSE (2.25 cm, SD: 0.31 cm) indicate that the Hall-effect sensor and PLC-based control architecture can maintain vehicle alignment with the magnetic guidance path under operating conditions. The 100% path-completion rate (15/15 trials) confirms the robustness of the navigation strategy within the framework.

The fail-safe evaluation showed that the vehicle stopped within 7.37 cm (SD: 0.76 cm) after path-loss detection, satisfying the safety requirement of less than 10 cm. This demonstrates the effectiveness of the proposed safety mechanism in the analytical model.

The relay-matrix selective route-activation architecture offers a meaningful technical advance over conventional passive magnetic-tape systems. By energizing only the electromagnets corresponding to the required route, the system reduces unnecessary power consumption, simplifies route management, and improves navigation reliability. This selective activation approach distinguishes the proposed system from prior work and is the primary technical contribution of this study.

The table below provides a quantitative comparison with representative prior systems. Unlike vision-based systems, which require significant computational resources, or LiDAR-SLAM systems which are cost-prohibitive for assistive applications, the proposed PLC-based magnetic guidance approach achieves sub-2 cm lateral tracking error at low computational cost.

Table 6. Quantitative Comparison with Representative Prior Navigation Systems

System	Navigation Method	Lateral Error	Hardware Cost (est.)	PWD Adapted	Reference
Proposed ATV	Magnetic + PLC	1.52 cm (sim.)	Low (~USD 500)	Yes	Current work
Su et al. 2018 [21]	Magnetic tracking	~2–5 cm	Low–Med	No	[21]
Zou et al. 2021 [25]	LiDAR SLAM	<5 cm	High (>USD 5000)	No	[25]
Vimalesh et al. 2024 [38]	RGB color-following ATV	~3–8 cm (est.)	Medium	No	[38]
Run & Xiao 2018 [40]	IR ceiling transmitters	~5 cm (est.)	Low	No	[40]
Sayemaldahar & Chauhdary 2021 [41]	Smart wheelchair (sensor array)	N/A (collision avoid.)	Medium	Yes	[41]

Overall, the findings suggest that the proposed approach provides a low-cost and reliable analytical foundation for autonomous indoor mobility assistance. The relay-matrix architecture, voice-command integration, and PWD-specific design represent meaningful contributions in the context of assistive robotics. Future work must focus on: user studies involving persons with disabilities; and (4) large-scale deployment scenarios.

5. Study Limitations

Drivers with musculoskeletal disabilities may not be able to personally deliver medicines or parcels directly into hospital rooms. However, they can knock on doors, call patients into the corridor, and transfer delivered items. Route guidance paths must be installed in advance and regularly maintained. Vehicle batteries require periodic charging, and routine maintenance must be performed. Oscillatory vehicle motion may increase electromagnet power consumption; vehicle speed should be reduced when this occurs.

6. Conclusions

This paper presents an Automated Transport Vehicle (ATV) for persons with disabilities, using magnetic-path navigation, Hall-effect sensors, PLC-based control, and electromagnetically assisted steering. The prototype design provides a cost-effective and practical alternative to more complex robotic navigation platforms while demonstrating reliable indoor navigation performance. The primary technical contribution is the relay-matrix selective route-activation architecture, which enables dynamic route reconfiguration without re-laying physical infrastructure, distinguishing this work from conventional passive magnetic-tape systems.

Results demonstrate a mean lateral tracking error of 1.52 cm, a 100% path-completion rate across 15 trials, and a mean fail-safe stopping distance of 7.37 cm, satisfying the design safety requirement of less than 10 cm.

The proposed ATV can enhance mobility and employment opportunities for blind, visually impaired, and mobility-impaired individuals by enabling transportation of tools, materials, and supplies within hospitals, factories, workshops, and other indoor facilities. The system contributes to improving independence, mobility, and social inclusion for persons with disabilities, in alignment with Saudi Vision 2030 goals. The concept may be extended to larger transportation environments, such as railway stations and public facilities, provided that suitable magnetic-guidance infrastructure is available.

References

1. World Health Organization. World report on disability 2011. WHO; 2011.
2. Al-Jadid MS. Disability in Saudi Arabia. Saudi Med J. 2013;34(5):453–60.

3. Welp A, et al. Making Eye Health a Population Health Imperative. Washington (DC): National Academies Press; 2016.
4. Tabbara KF, Ross-Degnan D. Blindness in Saudi Arabia. JAMA. 1986;255(24):3378–84.
5. Perna A, Proietti L. Musculoskeletal Rehabilitation: Current Challenges. J Clin Med. 2023;12(12):3981.
6. Trauzettel-Klosinski S. Current methods of visual rehabilitation. Dtsch Arztebl Int. 2011;108(51–52):871–8.
7. Altamirano J, et al. Disability Identity and Institutional Fairness. JAMA Netw Open. 2024;7(8):e2430367.
8. Ives-Rubley M, Khattar R, Roberts L. Removing Barriers for Workers with Disabilities. Center for American Progress. 2022.
9. Beneteau E, Feldner H, Pratt W. Employment experiences of adults with acquired disabilities. Disabil Rehabil Assist Technol. 2023;19:1–10.
10. Chen K-Y, Tsui C-Y. Fuzzy Control for a Quadruped Robot Guide Dog. Int J Fuzzy Syst. 2021;23:1789–1796.
11. Dicianno BE, et al. Systematic review: Automated vehicles for people with disabilities. Neurosci Lett. 2021;761:136103.
12. Karthick T, et al. Intelligent Guide Robots for People with Visual Impairment. Vision Rehabil Int. 2022;13(1):1–15.
13. Hwang J, Kim S. Autonomous vehicle transportation for people with disabilities. J Transp Geogr. 2023;106:103499.
14. Adagale V, Mahajan S. Robot Guide System for Blind People Using GPS and GSM. IJEEET. 2015;4(2):16–21.
15. Bateni H, Maki BE. Assistive devices for balance and mobility. Arch Phys Med Rehabil. 2005;86(1):134–45.
16. Salifu Y, Soar J, Hafeez-Baig A. Older people, assistive technologies, and barriers to adoption. Int J Med Inform. 2016;94:112–116.
17. Bennett R, Vijaygopal R, Kottasz R. Willingness of blind people to accept autonomous vehicles. Transp Res Part F. 2020;69:13–27.
18. Togizbayev BK, Omirzak S. Improving towing characteristics of aerodromic tow trucks. 2021.
19. Lee SY, Yang HW. Navigation of AGVs using magnet spot guidance. Robot Comput Integr Manuf. 2012;28(3):425–36.
20. Chan CY. Magnetic sensing as position reference for ground vehicle control. IEEE Trans Instrum Meas. 2002;51(1):43–52.
21. Su S, et al. Positioning accuracy improvement of AGVs via magnetic tracking. IEEE Intell Transp Syst Mag. 2018;12(4):138–48.
22. Yu X, et al. Positioning and navigation in an autonomous library robot using QR codes. Sensors. 2019;19(4):783.
23. Aparicio-Esteve E, et al. Combined infrared-ultrasonic positioning system. IEEE Sensors J. 2023;23(20):25152–64.
24. Xu Q, et al. Design of an ROS-based autonomous navigation system. IEEE ICMA. 2015:2220–2225.
25. Zou Q, et al. Comparative analysis of LiDAR SLAM-based indoor navigation. IEEE Trans Intell Transp Syst. 2021;23(7):6907–21.
26. Arafat MY, Alam MM, Moh S. Vision-based navigation for UAVs: Review and challenges. Drones. 2023;7(2):89.
27. Karimi MM, Mosavi MR. GPS/VIO integrated navigation based on factor graph and fuzzy logic. Sci Rep. 2024;14(1):30937.
28. Elsanhoury M, et al. Precision positioning for smart logistics using UWB. IEEE Access. 2022;10:44413–45.
29. Zhang HB, et al. Visual navigation of an AGV based on path recognition. IEEE ICMLC. 2004:3877–3881.
30. Buckham B, et al. Dynamics and control of a towed underwater vehicle. Ocean Eng. 2003;30(4):453–70.
31. Roy D, et al. Stochastic models for unit-load operations with autonomous vehicles. Ann Oper Res. 2015;231:129–55.
32. Madzharov D, et al. Integrating electric vehicles as flexible load in unit commitment. Energy. 2014;65:285–94.
33. Fuc P, et al. Environmental life cycle assessment of forklift operation. Int J Life Cycle Assess. 2016;21:1438–51.
34. Simpson RC. Smart wheelchairs: A literature review. J Rehabil Res Dev. 2005;42(4).
35. Reddy YK, et al. Electric Smart Scooter. Int Res J Eng Technol. 2020;7(06):1714–23.
36. Ranganeni V, et al. Levels of control for a navigation assistant for blind travelers. HRI. 2023:4–12.
37. [Reference to AI-powered visual-assistance tool, details omitted]
38. Vimalesh A, et al. Design and Development of AGV for Interior Logistics with Color-Based Navigation. ICRTC. 2024:393–406.
39. Channi HK, Kumar P, Dhingra A. Application of PLC in the Mechatronics Industry. 2024:185–209.
40. Run RS, Xiao ZY. Indoor autonomous vehicle navigation based on infrared technology. Appl Syst Innov. 2018;1(1):4.
41. Sayemaldahar MA, Chauhdary SH. An integrated smart wheelchair model. ICFNDS. 2021:93–99.
42. Alfahad OA, et al. An auto-adjusting algorithm to enhance indoor localization accuracy. IEEE Access. 2025;13:29739–53.
43. Zadeh LA, Aliev RA. Fuzzy Logic Theory and Applications. World Scientific; 2018.